Annals of Biomedical Engineering, Vol. 31, pp. 21–31, 2003
Printed in the USA. All rights reserved.

0090-6964/2003/31(1)/21/11/$20.00

Volume Currents in Forward and Inverse Magnetoencephalographic Simulations Using Realistic Head Models

ROBERT VAN UITERT, DAVID WEINSTEIN, and CHRIS JOHNSON

Scientific Computing and Imaging Institute, Department of Computer Science, University of Utah, Salt Lake City, UT

(Received 6 December 2001; accepted 12 November 2002)

Abstract—Volume currents are important for the accurate calculation of magnetoencephalographic (MEG) forward or inverse simulations in realistic head models. We verify the accuracy of our finite element method implementation for MEG simulations by comparing its results for spheres containing dipoles to those obtained from the analytic solution. We then use this finite element method to show that, in an inhomogeneous, nonspherical realistic head model, the magnetic field normal to the MEG detector due to volume currents often has a magnitude on the same order or greater than the magnitude of the normal component of the primary magnetic field from the dipole. We also demonstrate the disparity in forward solutions between a model that employs spheres, one that uses the realistic head and primary currents alone, and a realistic head model that incorporates both primary and volume currents. In forward and inverse MEG simulations using the inhomogeneous realistic model, the results obtained from calculations containing volume currents are more accurate than those derived without considering volume currents. © *2003 Biomedical Engineering Society.* [DOI: 10.1114/1.1535412]

Keywords—Magnetoencephalography, Source localization, Finite element method.

INTRODUCTION

Extracranial magnetic fields produced by neuronal activity within the brain can be measured using magnetoencephalography (MEG). A standard method for modeling the macroscopic neural activity assumes that such activity can be modeled by electric current dipoles. The electric currents produced by the dipoles can be separated into two components: the primary current, which represents the source of neural activity, and the secondary or volume current, which results from the interaction of the primary current within a conductive medium.[9,10] MEG detectors measure the normal component of the net magnetic field due to both primary and secondary currents.

Attempts to determine the magnetic fields that result from current dipoles, the forward problem, most commonly use a model for simulations consisting of a set of concentric spheres, each with homogeneous and isotropic conductivity.[4,5] Given this model, the MEG forward problem can be reduced to a closed form analytic solution. However, with more realistic, inhomogeneous, nonspherical head models, a closed form solution cannot be computed and approximation methods, such as finite or boundary element methods, must be used.

In realistic head models, the importance of volume currents for forward simulation of the MEG measured magnetic field is still debated, even though prior work has implied their relevance for radially oriented dipoles.[6] We used the numeric linear and quadratic finite element methods[2,3,7,13,14,18] to investigate the effects that volume currents have on the total magnetic field measured at the MEG detectors, and their importance in accurately calculating the normal component of the magnetic field detected by MEG. The accuracy of our numerical approximation is first validated by comparing the model's computed results for spheres containing dipoles to that of the analytic solution for the spheres. This numeric method is then applied to forward simulations in a more realistic head model.

The task of determining a current dipole's location within the head from the normal component of the magnetic field located at each detector, the inverse problem, or dipole source localization, relies on the techniques and modeling of the forward problem. After determining the importance of volume currents in the forward simulations, we used our forward model to perform inverse simulations on the realistic head model and demonstrate the importance of volume currents for accurate dipole source localization.

BACKGROUND

The dipole's primary current density, $\mathbf{J}_p$, results from the electromotive force impressed by biological activity on conducting tissues.[12] Assuming $\mathbf{J}_p$ is within a conductive region, G, of the brain with conductivity σ and that the magnetic permeability is homogeneous, $\mu = \mu_0$, the

Address correspondence to Chris Johnson, Scientific Computing and Imaging Institute, Department of Computer Science, University of Utah, Salt Lake City, UT 84112. Electronic mail: crj@sci.utah.edu

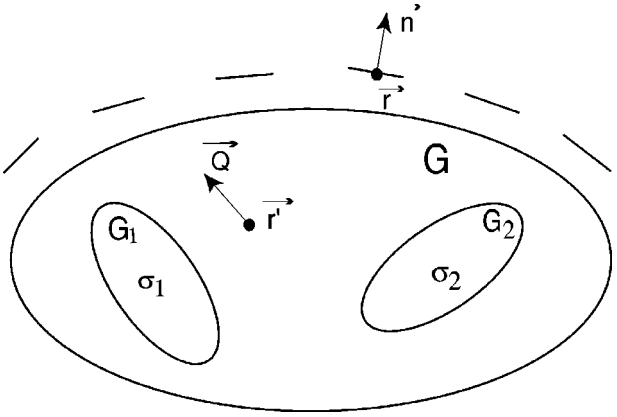

FIGURE 1. Schematic diagram showing the relationship between r′ (coordinate of the dipole), Q (moment of dipole), r (coordinate of the detector), n (normal to the detector), *G* (total conductive region), G_1 (conductive subregion 1), G_2 (conductive subregion 2), σ_1 (conductivity of subregion 1), and σ_2 (conductivity of subregion 2).

quasistatic approximations of Maxwell's equations in determining the electric field, **E**, and the magnetic field, **B**, apply as follows:

$$\mathbf{E} = -\nabla\phi, \tag{1}$$

$$\nabla\times\mathbf{B} = \mu_0\mathbf{J}, \quad \nabla\cdot\mathbf{B} = 0, \tag{2}$$

$$\mathbf{J} = \mathbf{J}_p + \sigma\mathbf{E}, \tag{3}$$

where ϕ is the electric potential and **J** is the total current density. The magnetic field is calculated by the Biot–Savart law:

$$\mathbf{B}(\mathbf{r}) = \frac{\mu_0}{4\pi}\int_G \mathbf{J}(\mathbf{r}')\times\frac{(\mathbf{r}-\mathbf{r}')}{|\mathbf{r}-\mathbf{r}'|^3}dv', \tag{4}$$

where $\mathbf{r}'$ is the coordinate of the dipole and **r** is the point of detection (Fig. 1). Combining Eqs. (1), (3), and (4), we obtain

$$\begin{aligned}\mathbf{B}(\mathbf{r}) &= \frac{\mu_0}{4\pi}\int_G [\mathbf{J}_p - \sigma\nabla\phi]\times\frac{(\mathbf{r}-\mathbf{r}')}{|\mathbf{r}-\mathbf{r}'|^3}dv' \\ &= \frac{\mu_0}{4\pi}\left[\int_G \mathbf{J}_p\times\frac{(\mathbf{r}-\mathbf{r}')}{|\mathbf{r}-\mathbf{r}'|^3}dv' - \Sigma\sigma_j\int_{G_j}\nabla\phi \right. \\ &\quad \left.\times\frac{(\mathbf{r}-\mathbf{r}')}{|\mathbf{r}-\mathbf{r}'|^3}dv'\right],\end{aligned} \tag{5}$$

where G_j indicates subvolumes with different conductivities. For a current dipole with a moment **Q**:

$$\mathbf{B}(\mathbf{r}) = \frac{\mu_0}{4\pi}\left[\mathbf{Q}\times\frac{(\mathbf{r}-\mathbf{r}')}{|\mathbf{r}-\mathbf{r}'|^3} - \Sigma\sigma_j\int_{G_j}\nabla\phi\times\frac{(\mathbf{r}-\mathbf{r}')}{|\mathbf{r}-\mathbf{r}'|^3}dv'\right]. \tag{6}$$

The integral portion of Eq. (6) models the volume currents that are dependent upon the conductivity and electric potential, whereas the balance on the right-hand side of Eq. (6) models the primary current.

If the conductor is in the shape of a sphere, an analytic closed form equation exists for calculating the magnetic field. According to Sarvas,[12] the magnetic field outside of a homogeneous sphere enclosing a dipole can be calculated as follows:

$$\mathbf{B}(\mathbf{r}) = \frac{\mu_0}{4\pi F^2}(F\mathbf{Q}\times\mathbf{r}' - \mathbf{Q}\times\mathbf{r}'\cdot\mathbf{r}\nabla F), \tag{7}$$

where

$$F = |\mathbf{a}|(|\mathbf{r}||\mathbf{a}| + |\mathbf{r}|^2 - \mathbf{r}'\cdot\mathbf{r}),$$

$$\mathbf{a} = \mathbf{r} - \mathbf{r}',$$

$$\begin{aligned}\nabla F = &(|\mathbf{a}|^2/|\mathbf{r}| + \mathbf{a}\cdot\mathbf{r}/|\mathbf{a}| + 2|\mathbf{a}| + 2|\mathbf{r}|)\mathbf{r} \\ &-(|\mathbf{a}| + 2|\mathbf{r}| + \mathbf{a}\cdot\mathbf{r}/|\mathbf{a}|)\mathbf{r}'.\end{aligned}$$

Equation (7) shows that for a spherical conductor, if the source is oriented radially to the point where the magnetic field is being measured, then the system is a magnetically silent volume conductor.[4] Note that Eq. (7) does not directly include the conductivity, σ. In a homogeneous sphere the contribution to the magnetic field from the volume currents is independent of conductivity, though the volume currents are implicitly incorporated in Eq. (7) and do contribute to **B**, the total magnetic field.[12]

The detectors used in MEG measure only the component of the magnetic field normal to the detectors.[8] Thus, Eq. (6) becomes

$$\begin{aligned}\mathbf{B}(\mathbf{r})\cdot\mathbf{n} = \frac{\mu_0}{4\pi}\left[\mathbf{Q}\times\frac{(\mathbf{r}-\mathbf{r}')}{|\mathbf{r}-\mathbf{r}'|^3}\cdot\mathbf{n}\right. \\ \left. - \Sigma\sigma_j\int_{G_j}\nabla\phi\times\frac{(\mathbf{r}-\mathbf{r}')}{|\mathbf{r}-\mathbf{r}'|^3}dv'\cdot\mathbf{n}\right],\end{aligned} \tag{8}$$

where **n** is the normal to the detector. Equation (7) then becomes

$$\mathbf{B}(\mathbf{r})\cdot\mathbf{n} = \frac{\mu_0}{4\pi F^2}(F\mathbf{Q}\times\mathbf{r}' - \mathbf{Q}\times\mathbf{r}'\cdot\mathbf{r}\nabla F)\cdot\frac{\mathbf{r}}{|\mathbf{r}|}. \tag{9}$$

Equation (9) indicates that when the detectors are oriented radially to a spherically symmetric homogeneous conductor, MEG is sensitive only to the component of the primary electric current tangential to the sphere at the detector for any dipole inside the sphere; the radial component of the primary electric current does not contribute to the external magnetic field.[5,8] The volume currents also do not contribute to the measured magnetic values in a spherically symmetric homogeneous conductor as shown by Sarvas.[12]

RESULTS

In our simulations, the linear finite element method was used to calculate the electric potential in (1) a discrete, numeric model employing spheres and (2) in a model using realistic geometry from patient data.[16] The biomedical problem solving environment (BioPSE)[1] was used to solve the forward and inverse MEG simulations.

Spherical Head Model

Several tests were performed to validate the finite element approximation to Eqs. (7) and (9). Using a sphere, we calculated the magnetic field by our numeric model and compared it to the magnetic field calculated by analytic Eq. (7). The sphere tests were performed on a 98,001 node, 100 mm sphere centered at the origin containing 459,784 uniformally spaced tetrahedral elements with 180 detectors placed symmetrically around the sphere at radii of 130, 140, 150, and 160 mm. A dipole was placed first at the center of the sphere with a moment of (0, 0, 1000) nA m. In comparing the numeric to the analytic solution, the cumulative rms error of the magnitude of the magnetic field at all the detectors was 1.12×10^{-17} T. Solution magnitudes range from 2.2×10^{-12} to 5.0×10^{-14} T.

A dipole was next placed in the sphere at (80, 50, 0) mm with moment (1000, −500, 0) nA m. The results from the numeric model were compared to the calculations from Eq. (7) and were found to correspond with a relative rms error of 4.31×10^{-3}. Figure 2 allows for a visual comparison between the analytic and numeric magnetic fields calculated at the 180 detectors for this dipole.

The next validation test employed dipoles that were randomly placed and randomly oriented in the sphere. Only one dipole was inside the sphere for each of the numeric and analytic magnetic field calculations, and each of these was evaluated for all 180 detectors. The calculations were performed for 100 different dipoles.

First, only the radial component of the numerically calculated magnetic field solutions with and without the volume currents was compared to the radial component

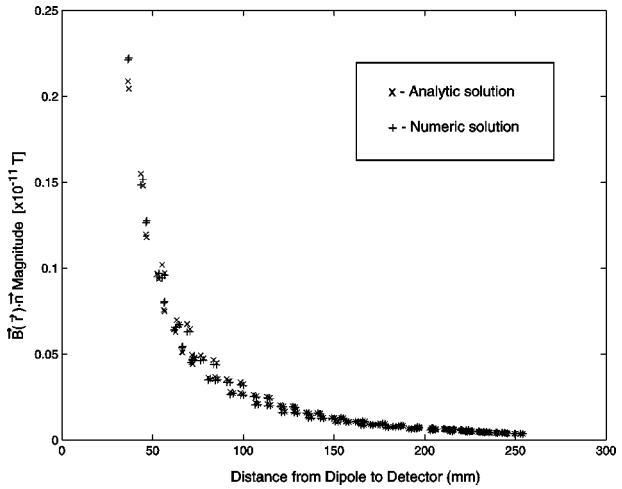

FIGURE 2. Analytic and numeric solutions of magnitude of magnetic field at detectors for dipole at (80, 50, 0) mm with moment (1000, −500, 0) nA m: x's indicate analytic solution, and crosses indicate numeric solution. The relative rms error between the analytic and numeric solution is 4.31×10^{-3}.

of the analytically calculated magnetic field solutions as calculated by Eq. (9). The relative rms error between the calculated radial component of the magnetic field for numeric and for analytic solutions for each dipole appears in Fig. 3; all errors were less than or equal to 0.156. The minimal difference between solutions with and without volume currents indicates that the radial component of the magnetic field due to the volume currents is close to zero in the sphere.

Using the same 100 dipoles, numerically calculated magnetic field solutions with and without the volume currents were then calculated for the total magnetic field

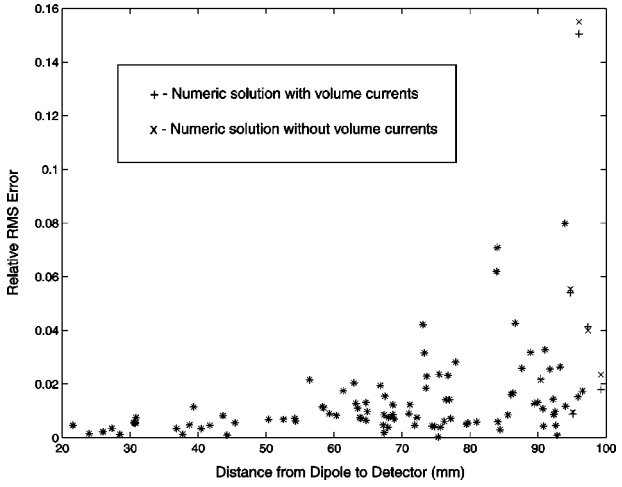

FIGURE 3. Relative rms error vs. distance from dipole to sphere center for radial component of magnetic field (100 randomly placed and oriented dipoles): crosses indicate numeric solution with volume currents, and x's indicate numeric solution without volume currents.

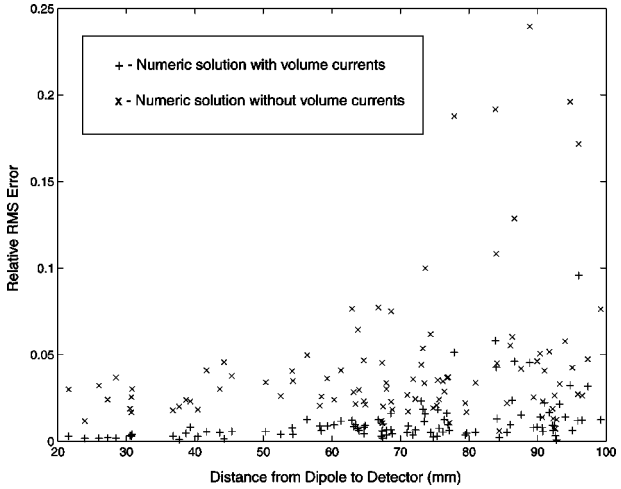

FIGURE 4. Relative rms error vs distance from dipole to sphere center for total magnetic field (100 randomly placed and oriented dipoles): crosses indicate numeric solution with volume currents, and x's indicate numeric solution without volume currents.

and compared to the analytically calculated magnetic field solutions. The mean relative rms error with the volume currents was 0.012 ± 0.014, with 91% of the dipoles having an error less than 0.024 and none having an error greater than 0.095 (Fig. 4). The relative rms error for numeric magnetic field solutions calculated without considering volume currents was 0.044 ± 0.042, with 71% of the dipoles having an error greater than 0.024. The errors for each dipole with and without the volume currents appear in Fig. 4. A discrepancy in accuracy between solutions including volume currents and those without volume currents is apparent when calculating the total magnetic field that was not evident when measuring the radial component alone. For each individual dipole, the relative rms error for solutions without the volume currents invariably was higher than was the error for those with the volume currents.

Realistic Head Forward Simulation

Next, we used the linear finite element method to calculate the MEG forward simulation as calculated by Eq. (8). The realistic head model used consists of 72,745 nodes, 406,493 uniformally spaced tetrahedral elements, and 64 detectors placed over the head in the standard electroencephalographic locations (Fig. 5). This model was constructed from a volume magnetic resonance image (MRI) scan of a 34 year old patient whose head had a radius of approximately 100 mm. We considered six conductivity regions and assigned them average values from the literature: air ($\sigma = 0.0$ S/m), skin ($\sigma = 1.0$ S/m), bone ($\sigma = 0.05$ S/m), CSF ($\sigma = 4.62$ S/m), gray matter ($\sigma = 1.0$ S/m), and white matter ($\sigma = 0.43$ S/m).[11]

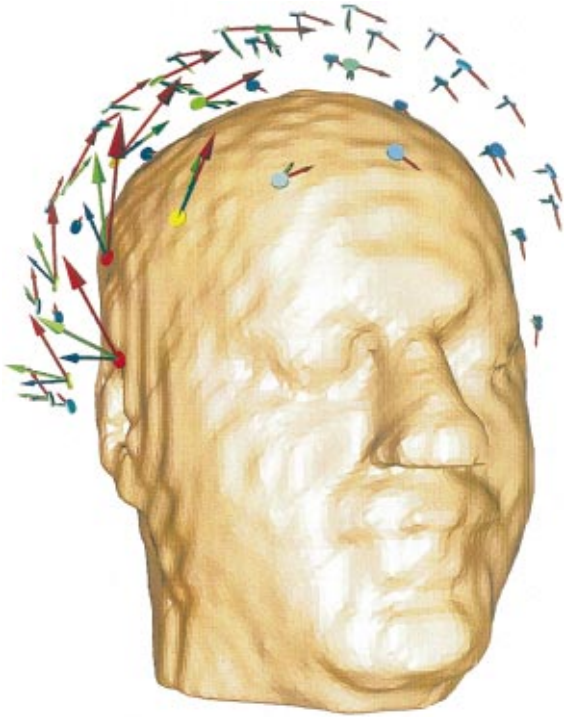

FIGURE 5. Magnetic field detector positions in the realistic head model. Detector color indicates the relative field strength of the measured magnitude of the magnetic field. A green arrow indicates the magnetic field calculated using both the primary and volume currents in the realistic head model. A red arrow indicates the magnetic field calculated using only the primary current in the realistic head model. A blue arrow indicates the magnetic field calculated using both the primary and volume currents in the spherical head model.

A dipole with moment (0, 0, -1200) nA m was located in the left parietal lobe at (35.0, 23.0, -50.6) with coordinate distances measured in millimeters from the origin at the center of the head. At 77% of the detectors (49 of 64), the normal component of the magnetic field due to the volume currents was of the same order of magnitude or larger than the normal component of the magnetic field due to the primary current. At 13% of the detectors (8 of 64), the normal component of the magnetic field due to the volume currents was at least an order of magnitude greater than the normal component of the magnetic field due to the primary current. Figure 6 shows the magnitude of the magnetic field normal to the detector at each of the detector positions with the magnetic field due to the combined volume currents and the primary current, with the magnetic field due to the primary current alone, and with the magnetic field due to the volume currents alone. Detectors numbered 1–18 measure fields over the left frontal region, detectors numbered 19–29 were localized over the left parietal–occipital region and were the closest to the placement of the dipole in this trial, detectors numbered 30–41 were

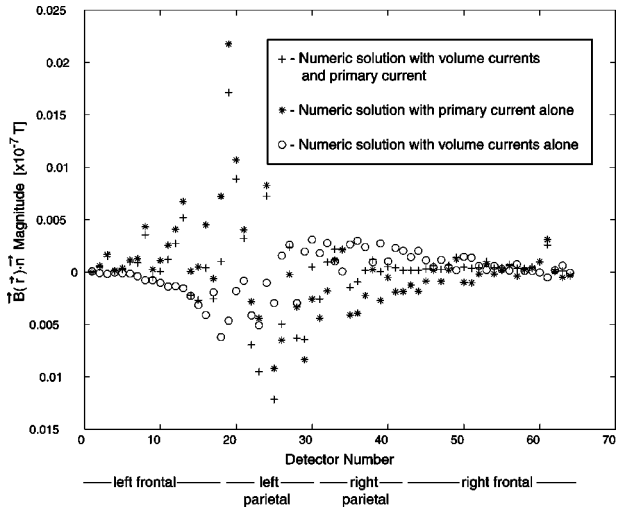

FIGURE 6. Normal component of the magnetic field for each detector with dipole in left parietal lobe of the brain: crosses indicate numeric solution with volume currents and the primary current, stars indicate numeric solution with the primary current alone, and circles indicate numeric solution with volume currents alone. Detector locations are noted below the detector numbers.

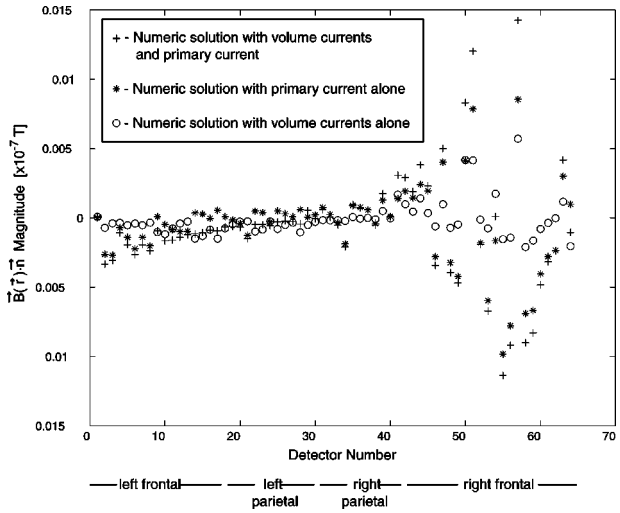

FIGURE 7. Normal component of the magnetic field for each detector with the dipole in the right posterior frontal cerebrum: crosses indicate numeric solution with volume currents and the primary current, stars indicate numeric solution with the primary current alone, and circles indicate numeric solution with volume currents alone. Detector locations are noted below the detector numbers.

placed over the right parietal–occipital region, and detectors numbered 42–64 were localized over the right frontal region and were the most remote from the dipole.

A dipole was also placed at $(-36.0, 4.0, 30.4)$ mm, in the right posterior frontal cerebrum, with a moment of $(0, 0, -1200)$ nA m. At 61% of the detectors (39 out of 64), the normal component of the magnetic field due to the volume currents was of the same order of magnitude or larger than the normal component of the magnetic field due to the primary current. At 16% of the detectors (10 out of 64), the normal component of the magnetic field due to the volume currents was at least an order of magnitude greater than that due to the primary current. Figure 7 shows the magnitude of the magnetic field normal to the detector at each of the detector positions with the magnetic field due to the combined volume currents and the primary current, with the magnetic field due to the primary current alone, and with the magnetic field due to the volume currents alone. The detectors for this simulation were at the same positions as were the detectors for the simulation with the dipole in the left parietal lobe.

In order to further verify the contribution of the magnetic field due to the volume currents is a real affect and does not have significant contributions from linear order finite element discretization errors, the above forward magnetic simulations on the realistic head model were calculated using a quadratic basis function.[13] For the dipole placed in the left parietal lobe, at 81% of the detectors (52 of 64), the normal component of the magnetic field due to the volume currents was of the same order of magnitude or larger than the normal component of the magnetic field due to the primary current; at 16% of the detectors (10 of 64), the normal component of the magnetic field due to the volume currents was at least an order of magnitude greater than that due to the primary current. For the dipole placed in the right posterior frontal cerebrum, at 58% of the detectors (37 of 64), the normal component of the magnetic field due to the volume currents was of the same order of magnitude or larger than the normal component of the magnetic field due to the primary current; at 17% of the detectors (11 of 64), the normal component of the magnetic field due to the volume currents was at least an order of magnitude greater than that due to the primary current. The relative rms error between the linear and the quadratic calculations of the normal component of the magnetic field was 3.9×10^{-3} for the dipole located in the left parietal lobe, and 3.0×10^{-3} for the dipole located in the right posterior frontal cerebrum.

Figure 8 relates the dipole location to the percentage of detectors recording the normal component of the magnetic field due to the volume currents as a number of the same order of magnitude or larger than the normal component of the magnetic field due to the primary current emanating from the dipole. Dipole location is expressed as the distance from the dipole to the nearest detector, a reflection of how ''deep'' the dipole is inside the head. The results suggest that the magnetic field due to volume currents plays a larger role in MEG for dipoles remote from the closest detector (i.e., deep inside the head) than for dipoles in the brain placed closer to the cranium.

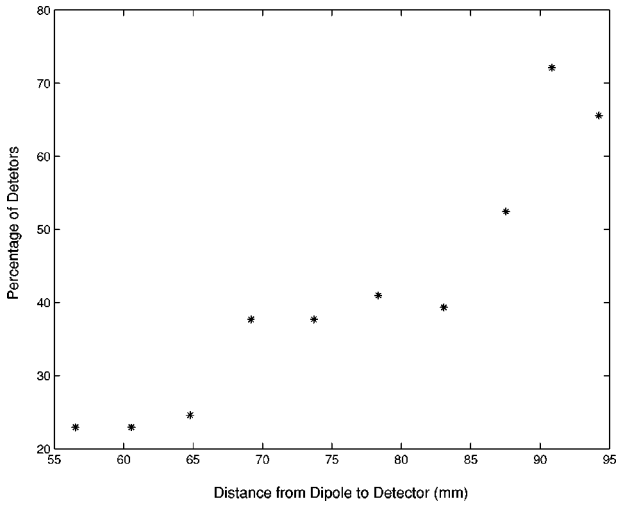

FIGURE 8. Percentage of detectors measuring magnetic field due to volume currents that are of the same order of magnitude or greater than the measured magnetic field due to the primary current at different dipole locations. Dipole location is expressed as the distance between the dipole and the nearest detector.

Even for dipoles close to the cranium, however, up to 22% of detectors measured magnetic fields due to volume currents of the same order of magnitude or greater than the fields due to the primary current.

Figure 9 shows the total magnetic field vector present at each detector position resulting from the dipole in the right posterior frontal cerebrum with the magnetic field due to the combined volume currents and the primary current in a realistic head model, with the magnetic field due to only the primary current in a realistic head model, and with the magnetic field due to the combined volume currents and the primary current in a spherical model that corresponds to the realistic head. In Fig. 10, each arrow is color coded to represent the MEG measured magnitude of the corresponding magnetic field vector in Fig. 9.

Realistic Head Inverse Simulation

The normal component of the magnetic field was calculated at each detector for a specific dipole using a forward simulation; the detectors' magnetic field data for this dipole, but not the dipole's location, was then used as the ''measured'' data with which to run an inverse MEG simulation. To avoid any bias in achieving the optimal results in the inverse simulations not using volume currents, no geometrical or measurement noise was added to the ''measured'' data. The inverse simulation was performed by positioning a test dipole in one element of the finite element head mesh, finding the minimum-norm solution magnitude and orientation for the dipole in that element, and then computing the misfit between the forward solution for the test dipole and the measured data.[15,17] The test dipole was then moved to different positions in the mesh until a position was found

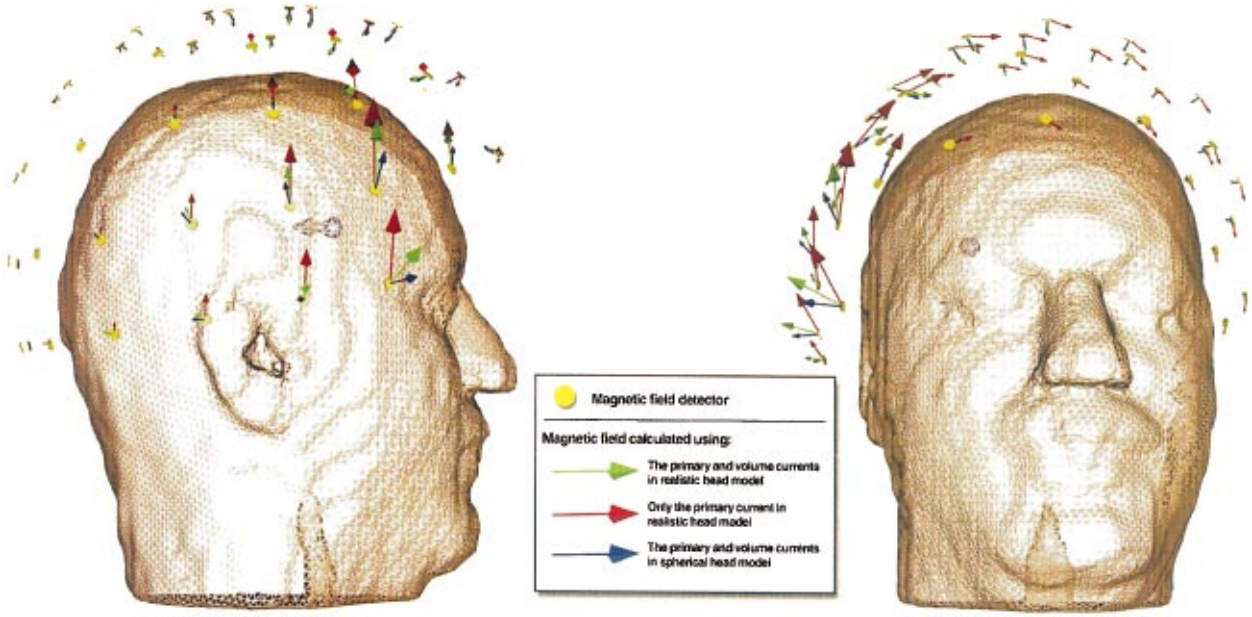

FIGURE 9. Total magnetic field vectors for each detector with the dipole in the right posterior frontal cerebrum: green indicates the magnetic field calculated using both the primary and volume currents in the realistic head model, and red indicates the magnetic field calculated using only the primary current in the realistic head model, and blue indicates the magnetic field calculated using both the primary and volume currents in the spherical head model. Detector locations are indicated by yellow disks.

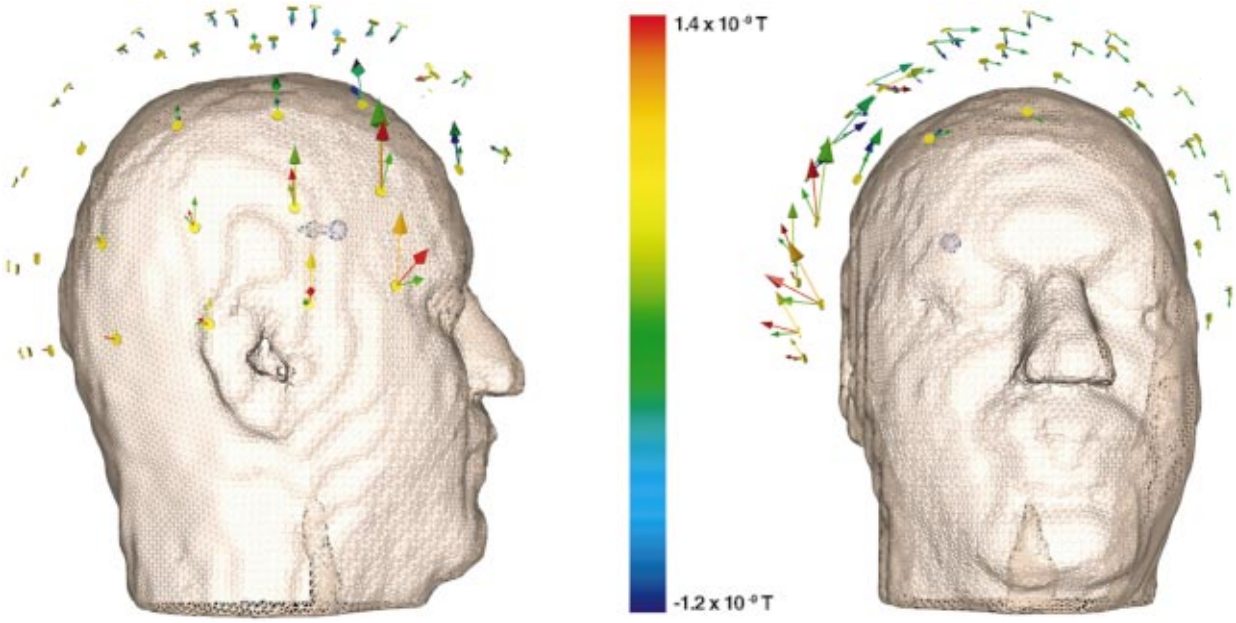

FIGURE 10. Magnitude of the normal component of the magnetic field for each detector with the dipole in the right posterior frontal cerebrum: the colors indicate the relative field strength of the measured magnitude of the magnetic field. Arrow directions correspond to magnetic field calculation vectors in Fig. 9 at the equivalent detectors.

where the misfit between the forward solution for the test dipole and the measured data was minimized. Rather than calculating the misfit between the forward solution for each test dipole position and the measured solution in each element, we used the downhill simplex[10] optimization search technique, which requires the evaluation of fewer elements to find the position where the minimum misfit occurs between the forward calculated solution and the measured solution.

Inverse MEG simulations were performed on data measured at detectors for ten different dipole locations within our realistic head model. Two sets of simulations were run: one set took into account the magnetic fields due to both the primary and volume currents, and the other set used only the magnetic field resulting from the primary current and ignored that due to the volume currents (Table 1). In all simulations, the initial dipole positions for the optimization were the same for both the calculation performed with and without the volume currents and the average of ten trials from different initial dipole positions is reported. Figures 11 and 12 show the dipole source localization points for the inverse solutions obtained using the measured data for a dipole at location C (35.0, 23.0, −50.6) mm in the left parietal lobe of the brain; the magnetic field for only the primary current was used to obtain the dipole position at location A, whereas the magnetic fields for both the primary and volume currents were used to obtain the dipole position

TABLE 1. Error in inverse localization calculations including and excluding the magnetic field due to volume currents.

Trial No.	Dipole coordinates and location in brain	Error with volume current magnetic field	Error without volume current magnetic field
1	(−36.0,4.0,30.4) right posterior frontal	1 mm	12 mm
2	(35.0,23.0,−50.6) left parietal	3 mm	62 mm
3	(35.0,−3.0,49.4) left frontal	6 mm	8 mm
4	(−15.0,−23.0,−0.6) right temporal	1 mm	8 mm
5	(−15.0,−23.0,−0.6) right temporal[a]	7 mm	46 mm
6	(−36.0,−23.0,−50.6) right parietal	2 mm	76 mm
7	(−15.0,47.0,−0.6) right precentral gyrus	4 mm	4 mm
8	(−15.0,−63.0,−50.6) right occipital	1 mm	14 mm
9	(27.0,51.0,11.4) left midfrontal	2 mm	4 mm
10	(−45.0,27.0,11.4) right midfrontal	1 mm	4 mm

[a]Different orientation from trial 4 right temporal dipole.

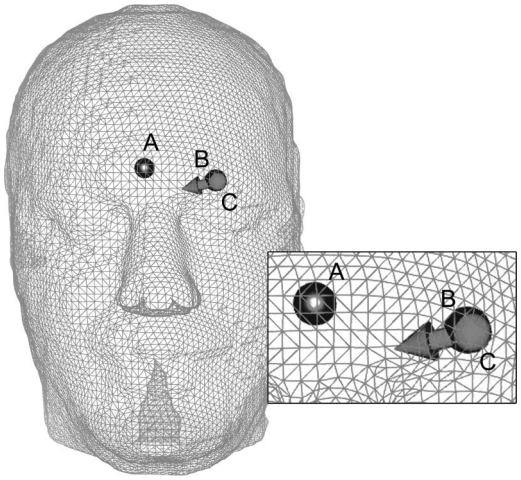

FIGURE 11. Dipole locations calculated by inverse MEG simulation using measured data obtained from the dipole positioned at (35.0, 23.0, −50.6) mm in the left parietal area: dark colored dipole A is the position calculated using the magnetic field due to the primary current alone, dark colored dipole B is the position calculated using magnetic fields due to both primary and volume currents, and light colored vector dipole C is the true dipole position.

at location B. In the ten dipole source localizations, 30% (3 of 10) of the localizations performed without volume currents resulted in a solution inaccurate by 6 mm or less, whereas 90% (9 of 10) of the localizations performed using the magnetic fields due to both primary and volume currents were within 6 mm of the correct dipole location. The average error in correctly identifying the dipole location for trials that included the magnetic field due to volume currents was 2.8 ± 2.1 mm; this error reflects discrepancies introduced by the simplex method, which does not exhaustively search every element. The average error for trials not taking into account the magnetic field due to volume currents was 23.8 ± 27.0 mm.

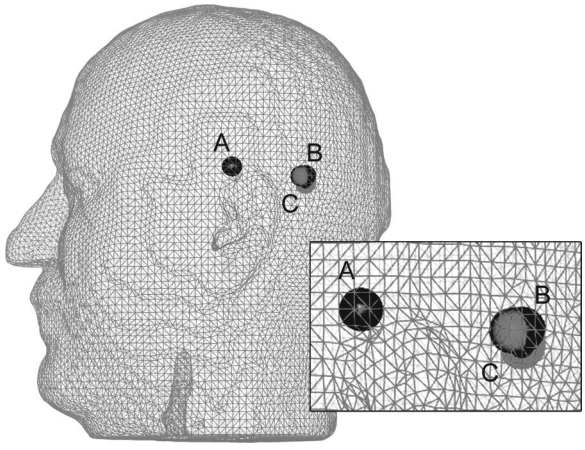

FIGURE 12. Left lateral view of the dipoles in Fig. 11: dark colored dipole A is the position calculated using the magnetic field due to the primary current alone, dark colored dipole B is the position calculated using magnetic fields due to both primary and volume currents, and light colored vector dipole C is the true dipole position.

DISCUSSION

The tests performed with the spheres and the comparison of the results with those obtained using the analytic solutions show that our numeric model is accurate. The rms error due to the dipole placed at the origin with moment (0, 0, 1000) nA m was only 1.12×10^{-17} T, whereas neuronal activity detected by MEG is on the order of 10^{-12}–10^{-14} T. The mean relative rms error of the 100 randomly placed and oriented dipoles was 0.012 ± 0.014; the errors that do occur stem from using a linear finite element approximation. The numeric model's accuracy is further confirmed by the results obtained with the dipole at (80, 50, 0) mm with moment (1000, −500, 0) nA m (Fig. 2). The detectors closest to the dipole location have the highest magnitude of magnetic field, whereas those farther away have a smaller magnitude, as would be expected. The numeric and analytic solutions have a relative rms error of only 4.31×10^{-3}.

Figure 3 shows the relative rms error between our model and the analytic solution when calculating the normal component of the magnetic field generated by randomly placed and oriented dipoles in a sphere. The error with and without the volume currents is the same except for 11 (out of 180) detectors; the error at these 11 detectors, the largest of which has a relative rms error of 0.154, is solely based on finite element approximation error. The errors increase as the distance from the center of the sphere increases because the spherical mesh employed was only an approximation containing an imperfect jagged boundary. The virtually identical results obtained with and without taking into account the volume currents is expected because, as demonstrated by Sarvas,[12] the normal component of the magnetic field measured at any detector on a sphere results from only the tangential component of the primary current and does not depend at all on the volume currents. In contrast to calculations involving only the radial component of the magnetic field, Fig. 4 clearly indicates that volume currents are important in total magnetic field calculations even in a spherical head.

The above tests demonstrate that our numeric model is reasonably accurate, and that the small inaccuracies that do occur result from the finite element approximation. Using a linear finite element method on a homogeneous, isotropic sphere is only a test case, however. The true usefulness of this technique becomes apparent when the method is applied to a realistic head that incorporates varying conductivities and for which an analytic solution is not available. The realistic model reemphasizes the importance of volume currents in MEG calculations, as

at least 22% of the detectors, and as many as 81% of the detectors, in our model measured magnetic fields due to volume currents that had magnitudes as large as or greater than the magnetic fields due to the primary current, and at least 13% of the detectors measured magnetic fields due to volume currents that were over an order of magnitude greater than the magnetic fields due to the primary current. These results were confirmed with the use of the more accurate quadratic finite element method and further emphasize the importance of the volume currents in MEG calculations. The relative rms error between the linear and quadratic finite element methods for the normal component of the magnetic field suggests that the frequent finding of the large magnetic field due to volume currents relative to the field from the primary currents is not just an anomaly of the linear finite element method.

Figures 6 and 7 show the importance of using volume currents when calculating magnetic field strengths in realistic head models. In Fig. 6, the increase in absolute magnitude of the calculated magnetic field occurred at detector numbers 10–29, which were located on the left parietal portion of the head and were closest to the dipole location. Similarly, the increase in the absolute magnitude of the calculated magnetic field at detector numbers 42–64 in Fig. 7 reflect the fact that these detectors were located on the right posterior frontal portion of the head and were closest to the dipole in this trial. In accord with the Biot–Savart law (4), the positive or negative magnitude of the magnetic field at each detector depends on the position of the detector with respect to the dipole. Figures 6 and 7 show that, for detectors close to the location of a dipole, the magnitude of the magnetic field would be calculated incorrectly for both positive and negative orientations if only the magnetic fields due to the primary current were included. In Fig. 6, detectors remote from the dipole location, such as detector numbers 37–51, generally have positive magnetic fields due to volume currents and negative fields resulting from the primary current. If the volume currents were not included in the calculation for these detectors, the total magnetic field measured at these detectors would appear to be negative rather than close to zero as would be expected for detectors in the right frontal region of a brain containing a left parietal dipole. Detectors numbered 19–29 in Fig. 7 also show that, for detectors remote from the dipole, calculations using both the volume and primary currents yield a result closer to the expected near-zero-field strength than do calculations using the primary current alone. At each extracranial detector in our realistic head model, Figs. 9 and 10 show that the magnetic field vectors and MEG measurements that include the magnetic field due to the volume currents differ greatly from those calculated using only the magnetic field due to the primary current; the magnetic field vectors and measured values for the spherical head model also are at variance with the corresponding vectors and values in the realistic head model regardless of whether or not volume currents were included in the calculation.

Accounting for the effects of volume currents in magnetic field calculations could be simplified and performed more selectively if the MEG measured magnetic field due to volume currents was of the same order of magnitude or greater than the measured field due to the primary current only at certain dipole locations, and if the measured field due to volume currents consistently was trivial at other dipole sites. Equation (8) implies that dipoles near a detector generally should produce magnetic fields with relatively low contributions from volume currents, since $|\mathbf{r}-\mathbf{r}'|^3$ appears in the denominator of the primary current portion of the equation and varies with dipole location, whereas $|\mathbf{r}-\mathbf{r}'|^3$ in the integral portion of the equation does not vary with dipole distance. Indeed, Fig. 8 suggests that dipoles placed superficially in the brain close to the cranium and near a detector have MEG measured contributions from volume currents that are of the same order of magnitude or greater than those from the primary current at only 22% of detectors, whereas dipoles placed deeper in the brain and remote from detectors produce measured magnetic fields from volume currents of the same order of magnitude or greater than those from the primary current at a higher percentage of detectors, up to 72% for the dipoles at a depth of 90.8 mm. Yet, Fig. 8 also indicates that even for superficially located dipoles, the contribution to the measured magnetic field from volume currents can still be large at some detectors when compared to the measured field from the primary current. Depending on the application, it appears one cannot automatically ignore the volume currents with confidence in magnetic field calculations for any dipole location in a realistic head model.

The inverse MEG simulations with dipoles at various positions within the realistic head model reemphasize the importance of the magnetic field due to volume currents in calculations designed for dipole source localization. 30% of the localizations performed without using the magnetic field due to volume currents obtained a solution inaccurate by 6 mm or less, whereas 90% of the localizations performed including the magnetic fields due to both the primary and volume currents were within 6 mm of the correct dipole location. Indeed, two simulations not using volume currents inaccurately localized the dipole to the wrong side of the head (trials 2 and 6 in Table 1). Figures 11 and 12 further illustrate this point by showing trial number 2 where a dipole that should be localized to the left parietal lobe, as shown in dipole B from a simulation using the magnetic fields due to both primary and volume currents, was localized to the right frontal lobe (dipole A) in a simulation that did not use

the magnetic field due to volume currents. These results demonstrate that if the magnetic field due to the volume currents is not used in inverse simulations, dipole source localization may be very inaccurate. These results also illustrate that the contribution of the magnetic field due to volume currents cannot be minimized as insignificant, but may be crucial for accurate source localization in realistic head models.

The necessity for including the magnetic field due to volume currents in inverse simulations in our model may seem obvious since the magnetic field due to volume currents was included in the forward simulation measured data. Yet, the importance of considering volume currents in inverse simulations is not diminished just because our model explicitly uses volume currents to calculate its measured data; Maxwell's Eqs. (1), (2), and (3) and the Biot–Savart law (4), which are fundamental to describing the magnetic fields emanating from a dipole, and must be incorporated into any realistic head model, intrinsically consider the magnetic field due to volume currents. Indeed, as these equations similarly apply to neuronal activity in actual human brain, attempts to localize a neural dipole in a human brain from MEG data also will require the use of the magnetic field due to volume currents in the calculations.

CONCLUSION

In homogeneous spheres, the contribution of volume currents to the magnetic field measured normal to MEG detectors may be ignored. However, for realistic head models the volume currents cannot be automatically disregarded. The head is not a sphere, and the volume currents do affect the magnetic field measured by MEG on the human head and in realistic inhomogeneous head models. In certain instances, the normal component of the volume currents can even have a greater affect than the primary current has on the measured magnetic field. The inclusion of the magnetic field due to volume currents gives more accurate solutions to the forward MEG problem and helps to more precisely localize neural sources in inverse MEG problems.

FUTURE WORK

Our current research involves investigating the importance of using realistic finite element head models, rather than spherical models, for forward and inverse MEG simulations. A validation of this work will be performed in collaboration with Richard Leahy of the University of Southern California on a phantom head model. We are also quantitatively studying the effect of conductivity values within the head on normal components of the magnetic field as measured by MEG, and how these conductivities influence both forward and inverse MEG simulations.

ACKNOWLEDGMENTS

This work was supported by NIH NCRR Grant No. 5P41RR012553-02. The authors would like to thank Nathan Galli for his assistance in generating the figures. The BioPSE software that was used for this research is available from our NIH NCRR center website: www.sci.utah.edu/ncrr

REFERENCES

[1] BioPSE: Biomedical Problem Solving Environment. Software available from the NIH Center for Bioelectric Field Modeling, Simulation, and Visualization: www.sci.utah.edu/ncrr
[2] Burnett, D. S. Finite Element Analysis: From Concepts to Applications. Reading, MA: Addison-Wesley, 1987.
[3] Chari, M. V. K., and S. J. Salon. Numeric Methods in Electromagnetism. San Diego: Academic, 2000.
[4] Gulranjani, R. M. Bioelectricity and Biomagnetism. New York: Wiley, 1998.
[5] Hämäläinen, M., R. Hari, R. J. Ilmoniemi, J. Knuutila, and O. V. Lounasmaa. Magnetoencephalography—Theory, instrumentation, and applications to noninvasive studies of the working human brain. *Rev. Mod. Phys.* 65:413–497, 1993.
[6] Haueisen, J., C. Ramon, P. Czapski, and M. Eiselt. On the influence of volume currents and extended sources on neuromagnetic fields: A simulation study. *Ann. Biomed. Eng.* 23:728–739, 1995.
[7] Jin, J. The Finite Element Method in Electromagnetics. New York: Wiley, 1993.
[8] Malmivuo, J., and R. Plonsey. Bioelectromagnetism: Principles and Applications of Bioelectric and Biomagnetic Fields. New York: Oxford University Press, 1995.
[9] Mosher, J. C., R. M. Leahy, and P. S. Lewis. Matrix kernels for the forward problem in EEG and MEG. Technical Report No. LA-UR-97-3812, Los Alamos National Laboratory, Los Alamos, NM 87545, 1997.
[10] Mosher, J. C., R. M. Leahy, and P. S. Lewis. EEG and MEG: Forward solutions for inverse methods. *IEEE Trans. Biomed. Eng.* 46:245–259, 1999.
[11] Peters, M. J., and J. C. De Munck. The influence of model parameters on the inverse solution based on MEGs and EEGs. *Acta Oto-Laryngol.* 491:61–69, 1991.
[12] Sarvas, J.. Basic mathematical and electromagnetic concepts of the biomagnetic inverse problem. *Phys. Med. Biol.* 32:11–22, 1987.
[13] Van Uitert, R., D. Weinstein, C. Johnson, and L. Zhukov. Finite element EEG and MEG simulations for realistic head models: Quadratic versus linear approximations. In: Proceedings of the 3rd International Symposium on Noninvasive Functional Source Imaging Within the Human Heart and Brain, edited by G. Fischer and F. X. Roithinger. Berlin: Springer, 2001, pp. 32–34.
[14] van den Broek, B. Volume conduction effects in EEG and MEG. Ph.D. thesis, University of Twente, Netherlands, 1997.

[15] Weinstein, D., L. Zhukov, and C. Johnson. Lead-field bases for electroencephalography source imaging. *Ann. Biomed. Eng.* 28:1–7, 2000.
[16] Weinstein, D. M., and C. R. Johnson. Effects of geometric uncertainty on the inverse EEG problem. In: Computational, Experimental, and Numerical Methods for Solving Ill-Posed Inverse Imaging Problems: Medical and Nonmedical Applications, edited by R. L. Barbour, M. J. Carvlin, and M. A. Fiddy. Bellingham, WA: SPIE, 1997, pp. 138–145.
[17] Zhukov, L., D. Weinstein, and C. Johnson. Independent component analysis for EEG source localization. *IEEE Eng. Med. Biol. Mag.* 19:87–96, 2000.
[18] Zienkiewicz, O. C., The Finite Element Method in Engineering Science. New York: McGraw-Hill, 1977.